

A CONSTRAINED HARTREE-FOCK MODEL FOR THE VAPORIZATION OF HOT NUCLEI

H. SAGAWA

National Superconducting Cyclotron Laboratory, Michigan State University, East Lansing, MI 48824-1321, USA

and

G.F. BERTSCH

*Department of Physics, University of Tennessee, Knoxville, TN 37996, USA
and Physics Division, Oak Ridge National Laboratory, Oak Ridge, TN 37831, USA*

Received 23 January 1985, revised manuscript received 5 March 1985

A new microscopic model is proposed to describe the expansion and vaporization of a hot nucleus. The model incorporates the dynamics of the expansion process into finite-temperature Hartree-Fock theory. Testing the method on ^{40}Ca , we find that most of the nucleus remains in the liquid phase if the temperature is below 8 MeV, and for higher temperatures most of it is turned to vapor in the initial expansion.

The theory of nuclear disassembly at high excitation energy is currently a topic of considerable interest [1–12]. Both statistical and dynamic models have been employed to describe the process. The initial expansion requires a calculation of dynamics such as given by mean field theory [7,8] or classical equations of motion [11]. In the final state, the clustering may well be described by an appropriate statistical theory [1–3]. We propose to solve a hybrid model that uses the dynamic equations of constrained mean field theory at finite temperature. We know that mean field theory works very well at nuclear matter density, and the finite-temperature generalization should be equally valid for the single-particle density matrix. Of course at low density, Hartree-Fock theory breaks down as clustering becomes important. However, we do expect our model to describe the separation of the system into a vapor and a liquid ⁺¹. Our aim will be simply to calculate the fraction of

nucleons that are left in the residual nucleus after the expansion phase, a quantity that might be experimentally accessible. That was also a goal of the calculations in ref. [6]. That work used a completely macroscopic model, whereas our method is microscopic.

A basic assumption of our model is that the system maintains global thermal equilibrium during the expansion. Thus it should be required that the thermal equilibration time scale be short compared to the expansion time scale. It is worth exploring that limit because the only other microscopic calculations that are presently possible demand the opposite limit [7,8]. Realistically the situation is in between, with the two time scales comparable.

In Hartree-Fock theory, systems can be studied away from dynamic equilibrium by adding constraining fields to the single-particle hamiltonian. To study the system as a function of density, fields of the form λr^2 and $\lambda \rho$ might be employed [15]. The Lagrange multiplier λ is chosen to give a minimum at the desired density. For our study, the basic physics left out the equilibrium description is the collective expansion

⁺¹ The presence of phase transition in nuclear matter between vapor and liquid phases may be taken for granted [13]. Whether or not it shows observable critical point behavior has been a subject of controversy [9–12,14].

of the hot system. This expansion takes energy from the thermal energy, and will affect the properties of the final state [4]. The collective energy of expansion can be included by constraining the system with a field proportional to the radial momentum, which we define by the operator $\frac{1}{2}(\mathbf{p} \cdot \mathbf{r} + \mathbf{r} \cdot \mathbf{p})$. It is convenient to use the operator r^2 to constrain the size of the system, because as will be seen below the operator relationship with $\mathbf{p} \cdot \mathbf{r}$ simplifies the calculations. In summary our model is based on the constrained Hartree–Fock theory with a hamiltonian

$$h'' = h_{\text{HF}}[\rho] - \lambda_1 r^2 - \lambda_2 \frac{1}{2}(\mathbf{p} \cdot \mathbf{r} + \mathbf{r} \cdot \mathbf{p}), \quad (1)$$

where λ_1 and λ_2 are independent Lagrange multipliers. The Hartree–Fock equations

$$h'' \phi_i = \epsilon_i \phi_i, \quad \rho = \sum_i (2j_i + 1) f_i(T) \phi_i^* \phi_i \quad (2)$$

may be derived from the hamiltonian by the variational principle for the thermodynamic potential of the grand canonical ensemble [16]. There is also a subsidiary condition to determine the particle number,

$$N = \sum_i (2j_i + 1) f_i(T) \\ = \sum_i \frac{(2j_i + 1)}{1 + \exp[(\epsilon_i - \mu)/T]}. \quad (3)$$

If the temperature is not too high, the Hartree–Fock equations have two sets of solutions depending on the starting conditions of the iteration process [14]. One set of wave functions is obtained by using the usual Woods–Saxon potential as an initial guess, while another set is obtained starting from zero potential. This latter is the vapor phase, while the former has a mixture of vapor and liquid.

Due to the radial momentum constraint, the hamiltonian h'' is complex (although of course hermitean) and will have complex eigenfunctions. We represent the hamiltonian by a tridiagonal matrix on a radial coordinate space mesh. The matrix is converted to a real symmetric matrix by applying a gauge transformation, and then the usual bisection method is used to find the eigenvalues and wave functions. For hamiltonians based on Skyrme-type interactions, this method appears to be somewhat faster than the commonly used Numerov algorithm [17].

To derive the dynamic equations of motion we

study the expectation values of the operators for the constraining fields. The equations of motion for these operators are given by

$$i d\langle r^2 \rangle / dt = \langle [r^2, h_{\text{HF}}] \rangle, \quad (4)$$

$$i d\langle \mathbf{p} \cdot \mathbf{r} \rangle / dt = \langle [\mathbf{p} \cdot \mathbf{r}, h_{\text{HF}}] \rangle, \quad (5)$$

where the expectation value implies averaging over the grand canonical ensemble

$$\langle O \rangle = \sum_i f_i(T) \langle \phi_i | O | \phi_i \rangle, \quad (6)$$

Eqs. (4) and (5) can be simplified if we express h_{HF} in terms of the constrained hamiltonian h'' and make use of the fact that h'' is diagonal. Then the commutators in eqs. (4), (5) only receive contributions from the constraining fields and we arrive at the following expressions

$$d\langle r^2 \rangle / dt = 2\lambda_2 \langle r^2 \rangle, \quad (7)$$

$$d\langle \mathbf{p} \cdot \mathbf{r} \rangle / dt = -2\lambda_1 \langle r^2 \rangle, \quad (8)$$

Before proceeding with a numerical study of these equations, let us see how they describe the dynamics of small amplitude motion. For small amplitudes we can assume that λ_1 and λ_2 depend linearly on the constrained expectation values,

$$\lambda_1 \cong \alpha (\langle r^2 \rangle - \langle r^2 \rangle_0), \quad \lambda_2 \cong \beta \langle \mathbf{p} \cdot \mathbf{r} \rangle, \quad (9)$$

and the two equations may be combined to yield

$$d^2 (\langle r^2 \rangle - \langle r^2 \rangle_0) / dt^2 \\ \cong -4\alpha\beta (\langle r^2 \rangle - \langle r^2 \rangle_0) \langle r^2 \rangle_0^2. \quad (10)$$

This equation shows that the system will oscillate with a frequency $\omega = 2(\alpha \cdot \beta)^{1/2} \langle r^2 \rangle_0$. This describes the giant monopole vibration at finite temperature, in the first sound limit. From the calculation below for ^{40}Ca we extract values of α , β which yield monopole frequencies of 22 MeV at $T = 2$ MeV, 9 MeV at $T = 4$ MeV and 6 MeV at $T = 6$ MeV. Thus for low temperature the first-sound monopole vibration has a frequency close to the zero temperature giant monopole. Hotter nuclei are softer with a lower monopole frequency. Similar conclusions were made in ref. [6] based on a macroscopic model of the finite temperature dynamics.

We now apply the constrained dynamic model to

the evolution of the nucleus ^{40}Ca for a range of temperatures. The Hartree–Fock calculations are based on the Skyrme hamiltonian SGII [18]. This hamiltonian has a density-dependent interaction proportional to $\rho^{1/6}$, giving a nuclear compressibility of $K_\infty = 218$ MeV and an effective mass $m^*/m \approx 0.7$. The saturation properties and collective excitations of many nuclei are well described by this hamiltonian. We solve the Hartree–Fock equations in a spherical box of radius $R = 12$ fm, taking 50 single-particle states both for neutrons and protons. The chemical potential is determined to keep the number of particles fixed at 40. This is somewhat different than ref. [14], in which the number of nucleons in the liquid phase is fixed. The initial temperature is arbitrary but then it must be allowed to vary to keep the excitation energy fixed during the expansion. Before studying the dynamic equations, we first give some results of the doubly constrained Hartree–Fock calculations. The dependence of the field expectations on the Lagrange multipliers is shown in fig. 1. We see that the radial momentum is very nearly linearly dependent on λ_2 , with a coefficient that increases with λ_1 . To understand this behavior, we note that the solution to the Hartree–Fock equations at finite λ_2 may be expressed in terms of the solution for $\lambda_2 = 0$. It is a straightforward algebraic exercise to show that the following relation holds for the wave functions

$$\phi_i(\lambda_1, \lambda_2) = \exp(i\lambda_2 \frac{1}{2}mr^2) \phi_i(\lambda_1 + \frac{1}{2}\lambda_2^2 m, 0), \quad (11)$$

The expectation value of $\mathbf{p} \cdot \mathbf{r}$ may then be evaluated as

$$\langle \mathbf{p} \cdot \mathbf{r} \rangle = \lambda_2 m \langle r^2 \rangle, \quad (12)$$

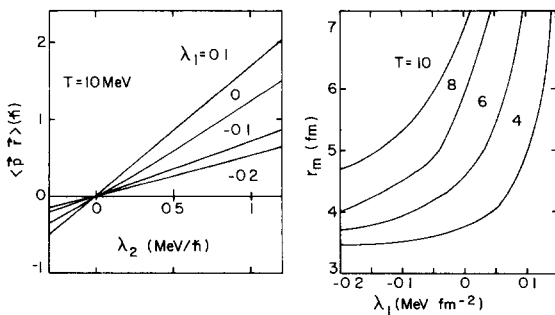


Fig. 1. The radial momentum $\langle \mathbf{p} \cdot \mathbf{r} \rangle$ at $T = 10$ MeV and the RMS radius r_m at $T = 4, 6, 8,$ and 10 MeV with respect to the Lagrange multipliers λ_1 (MeV fm $^{-2}$) and λ_2 (MeV fm $^{-1}$).

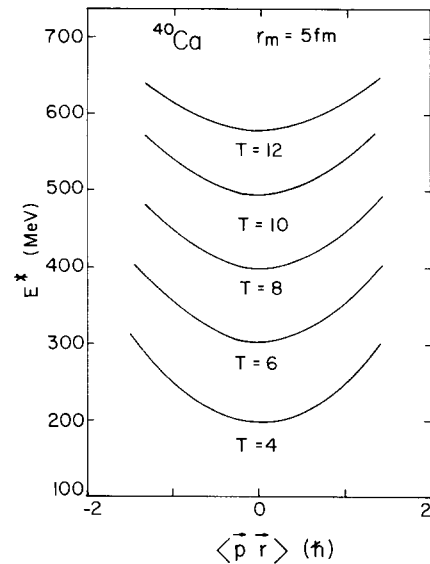


Fig. 2. The excitation energies E^* of ^{40}Ca at various temperatures as a function of the radial momentum $\langle \mathbf{p} \cdot \mathbf{r} \rangle$ for a fixed RMS radius $r_m = 5$ fm.

where $\langle r^2 \rangle$ is the expectation value in the state with $\lambda_2' = 0$, $\lambda_1' = \lambda_1 + \frac{1}{2}\lambda_2^2 m$. Since the term quadratic in λ_2 is small for values of physical interest, $\langle \mathbf{p} \cdot \mathbf{r} \rangle$ has a nearly linear dependence on λ_2 . In contrast, the RMS radius does not vary linearly with λ_1 . For low temperatures, the RMS radius increases slowly with λ_1 when the field is compressive, but increases rapidly for strong dilational fields. Pulling apart a nucleus that would be otherwise bound is a nonlinear process! Notice also that the RMS radius is almost independent of λ_2 . As noted above, that parameter changes primarily the phase of the wave function, keeping the density about the same. Some graphs of the excitation energy as a function of the constraining fields are shown in fig. 2. The energy is calculated as a function of λ_1 and λ_2 and then expressed in terms of the corresponding physical expectation values. The energy is a minimum at zero radial momentum and varies quadratically with that variable. In fig. 3 we show the entropy calculated from the grand canonical formula

$$S = - \sum_i (2j_i + 1) [f_i \ln f_i + (1 - f_i) \ln (1 - f_i)]. \quad (13)$$

We first compare the computed entropy with the Fermi gas model. For simplicity, let us assume that the Fermi gas occupies a sphere with the same RMS

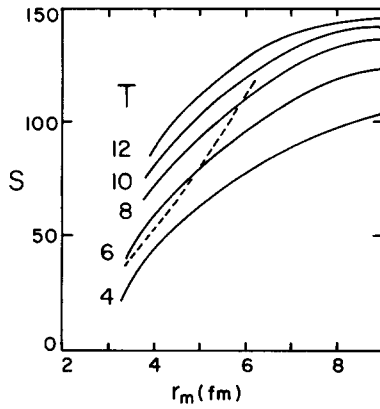


Fig. 3. The entropy S as a function of the radius r_m . The dashed curve shows the result of Fermi gas model calculation at $T = 6$ MeV performing numerically the derivative of the thermodynamic potential with respect to the temperature. Thus, higher order terms than eq. (14) are also included in the result.

radius as the calculated system. The entropy at low temperatures would then be given by

$$S \cong N \frac{1}{2} \pi^2 T / \epsilon_F = \pi^{4/3} \left(\frac{8}{9}\right)^{2/3} \frac{5}{3} r_m^2 m T N^{1/3}. \quad (14)$$

The Fermi gas entropy for $T = 6$ MeV is shown as the dashed line in fig. 3. It has about the right magnitude for moderately expanded nuclei. The deviation at large r_m is due to the limitation of the configuration space in the H-F calculation, while no limit to the

available phase space in the Fermi gas model. However, the calculated entropy for $r_m = 8$ fm only increases by 10% when the configuration space is doubled. Thus, the limitation of the configuration space does not have much effect on Hartree-Fock results, even at a high temperature such as $T = 12$ MeV. Note that the entropy is almost independent of the collective momentum $\langle p \cdot r \rangle$.

Our remaining initial conditions are to assume zero radial momentum, and that the mean square radius of the system corresponds to a nucleus near normal density. Whether this is realistic or not depends on the details of the process used to create the hot nucleus. For the calculation the initial conditions are imposed by starting the system with a negative λ_1 coefficient and $\lambda_2 = 0$. The time evolution of the hot system is determined from eqs. (7) and (8) using the results of the constrained Hartree-Fock calculations presented in figs. 1-3.

The results are shown in table 1 for two different values of the initial temperature, $T_1 = 6$ MeV and 12 MeV. The first point to note is that the entropy remains nearly constant during the expansion, although this was not imposed from the outset. Evidently our assumption, that the thermal equilibration time is small compared to the expansion time, insures that the motion is adiabatic in the thermodynamic sense. Of course it is essential that the model include the collective kinetic energy of expansion for the adiabatic behavior to occur. As noted in refs. [6] and [11], the

Table 1
Time evolution of the hot nucleus ^{40}Ca .

E^* (MeV)	t (fm/c)	λ_1 (MeV/fm ²)	λ_2 (MeV/ \hbar)	r_m (fm)	$\langle p \cdot r \rangle$ (\hbar)	T (MeV)	S	N_L (%)	N_V (%)
197	0	-0.10	0.0	3.90	0.0	6.0	57	92.0	8.0
	20	-0.03	0.78	4.07	0.31	5.5	58	89.0	11.0
	40	0.04	0.96	4.46	0.45	4.6	58	86.0	14.0
	60	0.09	0.52	4.84	0.29	4.0	59	82.0	18.0
	80	0.10	-0.24	4.93	-0.14	3.8	59	81.0	19.0
	100	0.06	-1.36	4.57	-0.62	4.2	59	84.0	16.0
597	0	-0.20	0.0	5.21	0.0	12.0	116	44.0	56.0
	20	-0.11	1.44	5.65	1.10	10.4	117	45.0	55.0
	40	0.01	1.7	6.80	1.85	7.3	117	38.0	62.0
	60	0.076	1.2	8.12	1.75	6.1	120	15.0	85.0
	80	0.11	0.37	8.90	0.7	5.9	121	3.0	97.0

entropy will increase when the system enters the region of phase instability, but this cannot be calculated without a detailed description of the clustering. Note also that the temperature decreases rapidly with time during the expansion process. Thus the physics of isothermal processes is not relevant to nuclear vaporization.

Another question of interest is how much of the system is left in a residual nucleus after the initial expansion has stopped. In macroscopic terms, there is a separation between a low and high density phase, the vapor and liquid. The two cases presented in table 1 show quite different behavior in this respect. For the case of $T_I = 6$ MeV, the attractive forces eventually stop the expansion, leaving a residual nucleus. This is seen by the decrease in r_m after a time $t = 80$ fm/c. In contrast, at $T_I = 12$ MeV the system is hot enough to expand indefinitely. These results are in accord with the conclusions of ref. [6], where the change from bound to unbound expansions was found to occur in the vicinity of $T_I = 8$ MeV.

The volume in which we allow the nucleons to move is too small to see a physical separation of the vapor and liquid phases, but we can determine the proportion of each by comparing with the density profile of the pure vapor solution of the Hartree–Fock equations at the same values of the Lagrange multipliers. Fig. 4 compares the physical density to

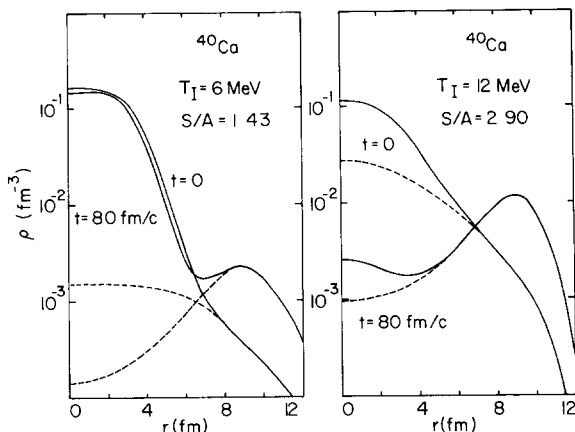


Fig. 4 The density distributions of ^{40}Ca at the initial and final stage of the expansion with the starting temperatures $T_I = 6$ and 12 MeV, respectively. The solid curves correspond to the total density with both liquid and vapor phases while the dashed curves show only the vapor phase.

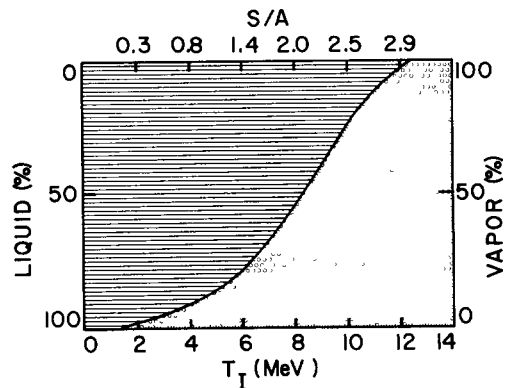


Fig. 5. The ratio of the mass number of the vapor phase to that of the liquid phase. The temperature T_I is that of the beginning of the expansion.

pure vapor solution and shows that there is enough of a difference to extract the vapor fraction. The proportion of nucleons in each phase is given in the last column of table 1. Thus we see that there is only about 20% vaporization at $T_I = 6$ MeV, but complete vaporization at $T_I = 12$ MeV. The vapor fraction is plotted as a function of temperature in fig. 5. The transition region is rather broad, of the order of 6 MeV as determined by the inverse slope of the curve in fig. 5.

We now turn to the measurable consequences of the disassembly behavior. To apply our results to physical observables, the results should be expressed in terms of the excitation energy rather than the temperature. Table 1 gives the excitation energy for the two cases we examined in detail, $E^* = 197$ MeV and $E^* = 605$ MeV. The first case might be achieved for example by a head-on collision of ^{20}Ne on ^{20}Ne at 25 MeV/n in the lab. An obvious consequence of the model is that there should be an evaporation residue left at rest in the CM frame for the lower energy collisions. The residue will of course be much smaller than the liquid portion we find at the end of the expansion, because of subsequent evaporation. But even at $T = 6$ MeV, the excitation energy of the evaporation residue is low enough so that most of the nucleons will remain in the final nucleus. The evaporation process needs to be studied more carefully with statistical cascade models to make quantitative predictions of the size of the final nucleus.

The theory predicts that there is a limiting temper-

ature in the formation of compound nuclei, as is discussed for example in ref. [19]. This might be observable in the energy spectra of light particles emerging from the collision. There may be found two components to the energy distribution, a high temperature component to be associated with the immediate vaporization and a lower temperature component from compound nucleus evaporation. There is some evidence [20] for a limiting temperature in heavy nuclei as high as 5 MeV; our calculations on a much smaller system would give a lower value. A compound nucleus is only formed at temperatures of 8 MeV and lower, and, as may be seen from table 1, there is considerable cooling in the initial expansion phase while the compound nucleus is forming.

This work is supported by the National Science Foundation under grant nos. PHY-83-12245 and PHY-84-13287 and by the Department of Energy under contract DE-AC05-84OR21400.

References

- [1] W.A. Friedman and W.G. Lynch, Phys. Rev. C28 (1983) 16.
- [2] J. Randrup and S. Koonin, Nucl Phys A356 (1981) 233.
- [3] A. Mekjian, Phys. Lett. 89B (1980) 177.
- [4] P. Siemens and J. Rasmussen, Phys. Rev. Lett. 42 (1979) 844.
- [5] G. Bertsch and P. Siemens, Phys. Lett. 126B (1983) 9.
- [6] H. Schultz et al., Phys. Lett. 147B (1984) 17.
- [7] A. Dhar and S. Das Gupta, Phys. Lett. 137B (1984) 303.
- [8] J. Knoll and B. Strack, Phys. Lett. 149B (1984) 45.
- [9] M. Curtin, H. Toki and D. Scott, Phys. Lett. 123B (1983) 289.
- [10] H. Jaqaman, A. Mekjian and L. Zamick, Phys. Rev. C29 (1984) 2067.
- [11] A. Vicentini, G. Jacucci and V. Pandharipande, University of Illinois preprint (1984).
- [12] A. Goodman, J. Kapusta and A. Mekjian, Phys. Rev. C30 (1984) 851.
- [13] U. Mosel, P. Zint and K. Passler, Nucl. Phys. A236 (1974) 252; W. Kuepper, G. Wegmann and E. Hilf, Ann. Phys. 88 (1974) 454.
- [14] P. Bonche, S. Levit and D. Vautherin, Nucl. Phys. A427 (1984) 278.
- [15] H. Sagawa and H. Toki, to be published.
- [16] D.J. Thouless, The quantum mechanics of many-body systems (Academic Press, New York, 1972).
- [17] M. Beiner et al., Nucl. Phys. A238 (1975) 29.
- [18] Nguyen van Giat and H. Sagawa, Phys. Lett. 106B (1981) 379.
- [19] S. Levit and P. Bonche, MIT preprint CTP 1214 (1984).
- [20] S. Song et al., Phys. Lett. 130B (1983) 14.